KI REPORTS
KIReports.org
TRANSLATIONAL RESEARCH

COL4A3 Mutation Induced Podocyte Apoptosis by Dysregulation of NADPH Oxidase 4 and MMP-2

Jun Tong[1,2], Qimin Zheng[1,2], Xiangchen Gu[1,2], Qinjie Weng[1], Shuwen Yu[1], Zhengying Fang[1], Hafiz Muhammad Jafar Hussain[1], Jing Xu[1], Hong Ren[1], Nan Chen[1] and Jingyuan Xie[1]

[1]Department of Nephrology, Institute of Nephrology, Shanghai Ruijin Hospital, Shanghai Jiao Tong University, School of Medicine, Shanghai, China

Introduction: Podocyte apoptosis is a common mechanism driving progression in Alport syndrome (AS). This study aimed to investigate the mechanism of podocyte apoptosis caused by *COL4A3* mutations.

Methods: We recruited patients with autosomal dominant AS (ADAS). Patients with minimal change disease (MCD) were recruited as controls. Microarray analysis was carried out on isolated glomeruli from the patients and validated. Then, corresponding mutant human podocytes (p.C1616Y) and 129 mice (p.C1615Y, the murine homolog to the human p.C1616Y) were constructed. The highest differentially expressed genes (DEGs) from microarray analysis were validated in transgenic mice and podocytes before and after administration of MMP-2 inhibitor (SB-3CT) and NOX4 inhibitor (GKT137831). We further validated NOX4/MMP-2/apoptosis pathway by real-time polymerase chain reaction (PCR), immunohistochemistry, and western blot in renal tissues from the ADAS patients.

Results: Using microarray analysis, we observed that DEGs, including NOX4/H_2O_2, MMP-2, and podocyte apoptosis-related genes were significantly upregulated. These genes were validated by real-time PCR, histologic analysis, and western blot in corresponding mutant human podocyte (p.C1616Y) and/or mice models (p.C1615Y). Moreover, we found podocyte apoptosis was abrogated and MMP-2 expression was down-regulated both *in vivo* and *in vitro* by NOX4 inhibition, urinary albumin-to-creatinine ratio, 24-hour proteinuria; and renal pathologic lesion was attenuated by NOX4 inhibition *in vivo*. Furthermore, podocyte apoptosis was attenuated whereas NOX4 expression remained the same by inhibition of MMP-2 both *in vivo* and *in vitro*.

Conclusion: These results indicated that NOX4 might induce podocyte apoptosis through the regulation of MMP-2 in patients with *COL4A3* mutations. Our findings provided new insights into the mechanism of ADAS.

Kidney Int Rep (2023) **8,** 1864–1874; https://doi.org/10.1016/j.ekir.2023.06.007
KEYWORDS: *COL4A3* mutation; NADPH Oxidase 4; MMP-2; Podocyte Apoptosis

ADAS is caused by heterozygous mutations in the *COL4A3/4*.[1] The frequency of pathogenetic mutations of *COL4A3/4* is reported as high as 1/106 in the general population based on a recent large sample size study.[2] In addition, pathogenic mutations in the *COL4A3/4* could lead to a range of phenotypes, including familial IgA nephropathy, focal segmental glomerulosclerosis (FSGS), thin basement membrane nephropathy, steroid-resistant nephrotic syndrome and familial chronic kidney disease.[3] For example, our recent study discovered heterozygous *COL4A3* mutations in 12.5% of FSGS families and 2% of sporadic FSGS patients.[4]

Podocytes, a key component of the glomerular filtration barrier, are exposed to permanent transcapillary filtration pressure and adhere tightly to the glomerular basement membrane (GBM). Type IV collagen is the major component of GBM. Reduction of *COL4A3-5* caused by pathogenetic mutations disrupt heterotrimer formation in podocytes; therefore, the mutant *COL4* can cause abnormal interaction with podocytes, and

Correspondence: Hong Ren or Chen Nan or Jingyuan Xie. Department of Nephrology, Institute of Nephrology, Shanghai Ruijin Hospital, Shanghai Jiao Tong University, School of Medicine, No 197, Ruijin Er Road, Shanghai 200025, China. E-mail: renhong66@126.com or cnrj100@126.com or nephroxie@163.com

[2]JT, QZ, XG contributed equally to this work.

Received 27 September 2022; revised 15 May 2023; accepted 5 June 2023; published online 19 June 2023

eventually podocyte apoptosis.[5,6] Furthermore, it is well known that podocyte apoptosis was increased in glomeruli of diabetic mice.[7,8] Gorin *et al*.[9] reported that inhibition of NOX4 reduced NOX4-dependent reactive oxygen species (ROS) generation and attenuated podocyte apoptosis in OVE26 mice, a model of type 1 diabetes.[10] And Zhou *et al*.[11] discovered that NOX2 inhibitor could attenuate podocyte apoptosis in type 2 diabetic nephropathy of db/db mice, suggesting NOX/ROS may play a role in podocyte apoptosis in *COL4* mutations. Our previous study[12] demonstrated that excessive endoplasmic reticulum stress (ERS) and ERS-induced apoptosis were involved in the podocyte injury caused by the NC1-truncated *COL4A3* mutation; MG132 (a proteasome inhibitor) intervention improved ERS-related podocyte apoptosis, indicating that ERS was also involved in podocyte apoptosis in *COL4A3* mutations. Autophagy has been reported to have a protective role against podocyte injury. Li *et al*.[13] reported that the level of autophagy was decreased in diabetic rats, and spironolactone inhibited mechanical-stress-induced podocyte injury partially through restoring autophagy activity.

Until now, there is no specific treatment for AS because the pathogenesis of GBM lesions and podocyte injury is still unknown. Therefore, we selected patients with ADAS caused by *COL4A3* heterozygous mutation, and we obtained DEGs through microarray analysis of transcripts from the isolated glomerulus, followed by functional analysis. Finally, we revealed that NOX4 might induce podocyte apoptosis through regulation of MMP-2 in patients with *COL4A3* mutations.

METHODS

Ethics Approval and Consent to enrollment

This study was performed following the Declaration of Helsinki and approved by the Ethics Committee of Ruijin Hospital, Shanghai Jiaotong University, School of Medicine. Written informed consent was obtained from each patient.

Patients

All patients enrolled in this study were recruited at the Department of Nephrology, Ruijin Hospital, Shanghai Jiaotong University, School of Medicine from 2012 to 2014. We recruited 3 patients with ADAS with pathogenetic heterogenous mutations on *COL4A3* identified by whole exome sequencing. Predicted pathogenic variants were identified based on the American College of Medical Genetics and Genomics criteria.[14] Renal biopsy was performed and FSGS lesions were detected under light microscopy and electronic microscopy. All the patients had a family history of nephropathy following autosomal dominant inheritance pattern. Patients with systemic diseases such as obesity (BMI >30); HIV-associated nephropathy; infection; reflux nephropathy; autoimmune diseases were excluded. The glomerular filtration rate (GFR) was evaluated using the Chronic Kidney Disease Epidemiology Collaboration. Chronic kidney disease stage for patients enrolled was evaluated according to the standard of the National Kidney Foundation.[15]

Microarray Analysis of Transcripts From Glomeruli

A total of 3 samples from patients with ADAS were included. For each kidney sample, cortical regions were selected using a scalpel, followed by isolation of single glomeruli under an eyepiece. RNA was extracted from the isolated glomeruli. For each qualified kidney specimen, more than 20 glomeruli were needed for RNA extraction (N:5); Only qualified RNA samples with RNA integrity values >7.0 and the RNA concentration >30 ng/μl were used for microarray analysis (N:3). Finally, 3 samples remained in our cohort. In addition, 5 patients with MCD without genetic mutation by whole exome sequencing were enrolled as the control group. Moreover, complementary DNA was obtained from total RNA through reverse transcription. The complementary DNA was fragmented, labeled, and hybridized onto gene chips (Microarray Gene 1.0, Affymetrix, Santa Clara, CA) according to the manufacturer's instructions. Affymetrix1 Expression Console Software (version 1.2.1) was used for microarray analyses.

Clinical Characteristics

All clinical variables at the time of renal biopsy were collected. Gender, age at biopsy, serum creatinine, estimated GFR (eGFR), uric acid, 24-hour protein excretion, urinary albumin-to-creatinine ratio, and serum albumin were recorded.

Immunofluorescence Staining of Glomerular *COL4A3*

After antigen retrieval and blocking, 5-mm kidney sections were incubated overnight at 4 °C with primary rabbit anti-COL4A3 (ab111742, Abcam, USA). After washing with phosphate buffered saline, the sections were incubated with FITC-conjugated goat antirabbit secondary antibodies at 37 °C in the dark for 1 hour. Images were captured with AxioVert A1 microscope (Zeiss, Germany) with a digital camera, and the positively stained area in the glomeruli was calculated using ImageJ 1.51k software (National Institutes of Health). First, the images were adjusted into 8-bit grayscale images. The glomerular regions were selected, then the optical density was calculated. Next, the positively stained areas in the glomeruli were selected and set

appropriately, the cells were counted; finally, the positively stained regions were calibrated, and both measurements were normalized to the glomerular areas.

Animal Experiments

Animal maintenance and intervention were approved by the Animal Care Committee of Ruijin Hospital, Shanghai Jiao Tong University School of Medicine. The genetic background of transgenic mice was 129. The animal model constructed by CRISPR/Cas9 technology was *Col4a3* C1615Y transgenic mice. This missense mutation corresponds to amino acid number 1616 in humans and was first found in an FSGS family receiving renal biopsy in our department. Protein sequence alignment verified the corresponding mutation to C1615Y in model mice. There were 4 mice in each group. Mice were bred with standard rodent chow food. Male mice were used in the experiments, and the weight difference was less than 10%. All mice received treatment at 8 weeks. MMP-2 inhibitor, SB-3CT (Selleckchem, USA) was administrated intraperitoneally for 6 days before sacrifice at the dosage of 50 mg/kg; NOX4 inhibitor, GKT137831 (Selleckchem, USA) was administrated gavage for 28 days before sacrifice at the dosage of 60 mg/kg. All animal experiments were approved by the Ethics Committee of Ruijin Hospital.

Metabolic and Physiologic Parameters

Before sample collection, mice were provided water ad libitum, and 24-hour urine was collected in metabolic cages at weeks 4, 8, 12, 16, and 20. The urinary albumin amount was measured using a Mouse Albumin enzyme-linked immunosorbent assay Quantitation Set (Bethyl Laboratories, Inc., Montgomery, TX, USA). The urinary creatinine concentration from the same sample was detected by the QuantiChromTM Creatinine Assay Kit (BioAssay Systems, Hayward, CA, USA) according to the manual's procedures. Eyelid vein blood was collected at weeks 12 and 20. The serum creatinine was measured using a Mouse Creatinine Assay Kit (Crystal Chem Inc., Downers Grove, IL, USA) according to the manufacturer's protocol.

Glomerulus isolation from renal biopsy, RNA extraction from the glomerulus, microarray analysis, and identification of DEGs were performed as reported previously.[16]

Validation With Real-Time PCR

For validation of microarray data, the top highest DEG (MMP-2) in patients with ADAS compared with patients with MCD were selected, and its related gene NOX4 was also selected. Total RNAs from the glomerulus were extracted by using Ambion RNAqueous-Micro Kit (Ambion, Texas, USA), according to the manufacturer's protocol. Complementary DNA was synthesized by using a High-Capacity complementary DNA Reverse Transcription kit with RNase Inhibitor (Applied Biosystems; Thermo Fisher Scientific, CA, USA). Real-time PCR was performed using the SYBR Green PCR Master Mix (Applied Biosystems; Thermo Fisher Scientific, CA, USA) and the StepOnePlus Real-Time PCR System (Applied Biosystems; Thermo Fisher Scientific, Inc, CA, USA).

We applied real-time PCR to verify the mRNA levels of the candidate genes, and the genes selected for real-time PCR validation wereisolated from additional 10 patients, including 3 patients with ADAS and 7 patients with MCD, who met the criteria of patient selection mentioned before. Data were analyzed using the $2^{-\triangle\triangle CT}$ method and are presented as fold changes relative to a control sample after normalization against the expression of housekeeping genes.

Western Blot Analysis

The levels of protein expression were detected by western blot analysis as described previously.[10] Protein samples were extracted using radio immuno precipitation assay lysis buffer on ice (Beyotime Biotechnology, Nantong, China). Then the lysates were separated by centrifugation at 12,000 rpm for 20 minutes at 4 °C after aspiration. The supernatants were collected, and the protein concentration was measured with Pierce bicinchoninic acid Protein Assay Kit (Thermo Scientific, USA). Equal amounts of protein samples were loaded and separated by sodium dodecylsulfate-polyacrylamide gel electrophoresis and then transferred to polyvinylidene fluoride membranes. The membranes were then blocked with 5% nonfat milk at room temperature for 1 hour followed by incubation with primary antibodies at 4 °C overnight. On the next day, membranes were incubated with secondary antibodies for 1 hour at room temperature. β-actin or glyceraldehyde-3-phosphate dehydrogenase were used as an internal standard for normalization.

Primary antibodies included: MMP-2 (ab92536, Abcam, USA), NOX4 (ab133303, Abcam, USA), Cleaved-Cas3 (#9661S, Cell Signaling Technology, USA), β-actin (ab8226, Abcam, USA), and glyceraldehyde-3-phosphate dehydrogenase (ab9485, Abcam, USA) were used as the control. HRP-conjugated secondary antibodies (antimouse IgG, #7076; antirabbit IgG, #7074, Cell Signaling Technology, USA) were applied. Bands were visualized using a SuperSignal West Femto kit (Pierce, IL, USA).

Measurement of Podocyte H_2O_2

Measurement of podocyte H_2O_2 was performed using the hydrogen peroxide assay kit (Beyotime, China) as

described previously.[9] H_2O_2 is capable of oxidizing ferrous ions (Fe^{2+}) to ferric ions (Fe^{3+}) for 30 minutes at room temperature, followed by forming a visible purple complex for downstream measurement. The content of H_2O_2 was detected under a microplate reader at a wavelength of 560 nm (Bio-Rad, USA).

Cell Culture and Treatment

Human wild type (WT) podocytes and transgenic podocytes were cultured in 1640 medium containing 10% fetal bovine serum. Then podocytes were incubated with NOX4 inhibitor, GKT137831 (final concentration 140 nmol/l) for 1 hour before harvest; and MMP-2 inhibitor SB-3CT (final concentration: 14 nmol/l) for 48 hours before harvest. All these inhibitors were solubilized in DMSO.

Immunohistochemistry Staining of MMP-2

Immunohistochemistry staining was performed on formalin-fixed and paraffin-embedded kidney sections following standard procedures. Sections were blocked in 2% goat serum in phosphate buffered saline for 1 hour at room temperature and then incubated with the primary antibody against MMP-2 (ab92536, Abcam, USA) at 4 °C overnight. The next day, sections were washed with phosphate buffered saline 3 times and then incubated with biotinylated secondary antibodies for 1 hour, followed by incubation with an avidin-biotin–peroxidase complex for diaminobenzidine substrate development using the ABC kit (Vector Laboratories, Burlingame, CA, USA) at room temperature. Images were captured using a Leica DM1000 microscope. Positive staining was processed using peroxidase-labeled streptavidin and a diaminobenzidine substrate. The control included a kidney section from an MCD patient.

Light Microscopy

Fresh kidneys were fixed in 4% paraformaldehyde, embedded in paraffin, followed by hematoxylin-eosin staining (HE) and washed for light microscopy, HE staining was observed under a light microscope.

Electron Microscopy

Renal cortical sections were isolated and immersed in 2% glutaraldehyde in phosphate-buffered solution (pH 7.4), followed by incubation with 2% osmium tetroxide in phosphate-buffered solution (pH 7.4) for 2 hours at 4 °C, stained with lead citrate and uranyl acetate. Finally, renal sections were viewed under a HT770 transmission electron microscope (Hitachi, Japan).

Statistical Analysis

Statistical analysis was done using SPSS (version 21.0, Chicago, IL, USA). Continuous variables characterized by normal distribution were presented as the mean ± SD, 2-tailed t-test was used to analyze data between 2 groups. Continuous variables with skewed distribution were described as the median (range) and compared using the Mann-Whitney U test. Categorical variables were presented as frequencies and were compared with the chi-squared test. Statistical significance was defined at $P < 0.05$. All of the experiments were repeated at least 3 times.

RESULTS

Clinical Parameters

A total of 3 patients with ADAS and 5 patients with MCD were enrolled in the discovery group for microarray analysis. Patients with ADAS had late age of disease onset (51.3 ± 1.5 vs. 22.2 ± 3.4 years, $P = 0.035$), increased serum creatinine (138.67 ± 45.55 vs. 64.80 ± 10.92 μmol/l, $P = 0.036$), decreased level of eGFR (61.01 ± 16.62 vs. 108.29 ± 34.25 ml/min per 1.73 m^2, $P = 0.004$), proteinuria (ln-transformed urine protein, −0.79 ± 0.74 vs. 1.59 ± 0.41, $P = 0.021$), urinary albumin-to-creatinine ratio (45.37 ± 37.57 vs. 445.82 ± 168.92 mg/mmol, $P = 0.008$), and increased serum albumin (38.67 ± 1.53 vs. 12.40 ± 5.32 g/l, $P = 0.0002$). The clinical characteristics of the patients enrolled for microarray analysis (discovery group) were summarized in Table 1. A total of 3 patients with ADAS and 7 patients with MCD were enrolled in the validation group. In the validation group, patients with ADAS are characterized by different levels of proteinuria. The pathogenicity of *COL4A3* mutations was scored using the American College of Medical Genetics and Genomics criteria, and all patients with ADAS in the discovery and validation groups were either Pathogenic or Likely Pathogenic. Detailed information of patients with ADAS is available in the online Supplementary Table S1. Patients with ADAS had decreased proteinuria (ln-transformed urine protein, 0.69 ± 0.41 vs. 1.90 ± 0.61, $P = 0.0005$),

Table 1. Clinical characteristics of patients with ADAS and patients with MCD in the discovery group

Variable	ADAS	MCD	*P*
Number	3	5	-
Male/Female	1/2	3/2	0.465
Onset age (yr)	51.3 ± 1.5	22.2 ± 3.4	0.035[a]
Serum creatinine, μmol/l	138.67 ± 45.55	64.80 ± 10.92	0.036[a]
Uric acid, μmol/l	534.00 ± 183.34	337.60 ± 89.24	0.081
eGFR, ml/min per 1.73 m^2	61.01 ± 16.62	108.29 ± 34.25	0.004[a]
24 hr UprV(g)	0.75 (0.18–1.17)	6.0 (3.63–9.59)	0.036[a]
Ln(UP)	−0.79 ± 0.74	1.59 ± 0.41	0.021[a]
Serum albumin, g/l	38.67 ± 1.53	12.40 ± 5.32	0.0002[a]
ACR, mg/mmol	45.37 ± 37.57	445.82 ± 168.92	0.008[a]

ACR, albumin-to-creatinine ratio; ADAS, autosomal dominant alport syndrome; eGFR, glomerular filtration rate; MCD, minimal change disease; 24 hr UprV, protein amount of 24 hours urine.
[a]$P < 0.05$.

urinary albumin-to-creatinine ratio (328.82 ± 180.70 vs. 430.15 ± 198.99 mg/mmol, $P = 0.013$), and increased serum albumin (35.17 ± 4.53 vs. 13.43 ± 1.33 g/l, $P = 0.0000003$), which was consistent with the tendency in the discovery group. However, patients with ADAS had increased serum uric acid (430.18 ± 79.39 vs. 323.29 ± 78.87 μmol/l, $P = 0.013$), and there was no significant difference in age at disease onset, serum creatinine, and eGFR between patients with ADAS and patients with MCD in the validation group, which was distinct from the finding in discovery group. Detailed clinical information of validation group is available in the online Supplementary Table S2.

Characterization of *COL4A3* Expression in Glomeruli of Patients With ADAS Who Are Carrying *COL4A3* Mutations

By examining the localization and expression of *COL4A3* by immunofluorescence, we found that collagen type IV α3 chain in the glomerulus was mainly expressed in podocytes and the GBM, and the expression level of α3 chain in the glomerulus was significantly decreased and discontinued in patients with ADAS carrying *COL4A3* mutations (Figure 1).

Characterization of *COL4A3*$^{C1615Y/C1615Y}$ Transgenic Mouse Model

We constructed *Col4a3*$^{C1615Y/C1615Y}$ transgenic mice. The expression of α3 chain decreased significantly in the renal cortex of the mutant mice (Figure 2a), and the sequencing plot of mutation was presented in Figure 2b. We also measured clinical parameters of transgenic mice at 28 weeks: urinary albumin-to-creatinine ratio increased obviously compared with WT mice, and decreased significantly after NOX4 inhibition; 24-hour proteinuria decreased after NOX4 inhibition. No significant difference of serum creatinine compared with WT group, and there was no obvious difference of serum creatinine in WT and transgenic group before and after NOX4 inhibition (Figure 2c–e). Real-time PCR validation showed that the expression of *Nox4* and *Mmp-2* mRNA was higher in mutant group compared with that in the WT group (Figure 2f). Light micrographs represented focal adhesion of glomeruli (red arrow), tubular cast (yellow arrow), interstitial inflammatory cell infiltration (yellow triangle) in transgenic group, and alleviation of pathologic lesion after *NOX4* inhibition in transgenic group (Figure 2g). Electronic microscopy suggested segmental thickening of GBM and effacement of podocyte foot process in *COL4A3*$^{C1615Y/C1615Y}$ transgenic mice, and *NOX4* inhibition attenuated pathologic lesion (Figure 2h).

Microarray Analysis

Glomeruli isolation was processed as reported previously.[11] Transcripts extracted from glomeruli were used for microarray analysis, and the heat map comparison of microarray data revealed a distinct pattern of transcripts between patients with ADAS and patients with MCD (Figure 3a). Furthermore, Kyoto Encyclopedia of Genes and Genomes and Gene Ontology were used to explore the DEGs. Gene Ontology analyses found that JAK-STAT signaling pathway was one of the top upregulated pathways, and Kyoto Encyclopedia of Genes and Genomes analyses indicated that the ROS pathway was upregulated in glomeruli of patients with ADAS (Figure 3b and c). Of all the DEGs, *MMP-2* was the highest upregulated gene in the ADAS group as compared to the MCD group.

Validation of *NOX4* and *MMP-2*

The top DEG, *MMP-2* and its related gene *NOX4* were chosen for further validation in 3 additional patients

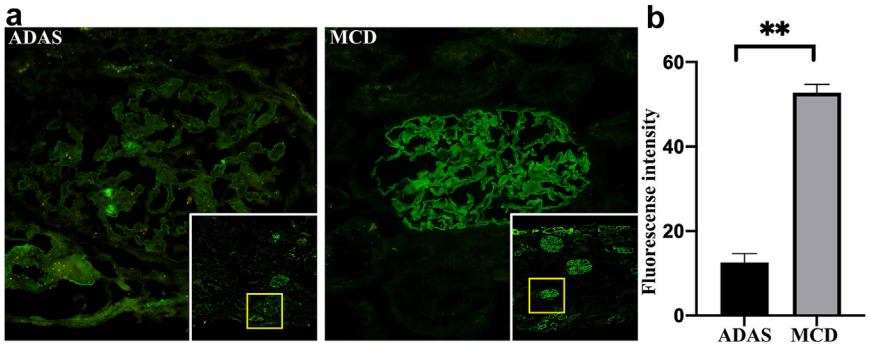

Figure 1. Type IV collagen α3 chain expression in glomeruli of patients with ADAS or MCD. (a) Expression of type IV collagen α3 chain in glomeruli of patients with ADAS and patients with MCD using immunofluorescence. Representative immunofluorescence image shows α3 chain expression in glomeruli of a ADAS patient caused by *COL4A3* mutation (p.C1616Y), and α3 chain expression in glomeruli of MCD patients as control. (b) Comparison of fluorescence intensity of α3 chain in glomeruli of patients with ADAS versus patients with MCD. Fluorescence intensity was calculated from 3 patients with ADAS and 5 control patients with MCD. The results are presented as the mean ± SEMs, 2-tailed *t*-test was used to analyze the data, $^{**}P < 0.01$.
ADAS, autosomal dominant Alport syndrome; MCD, minimal change disease.

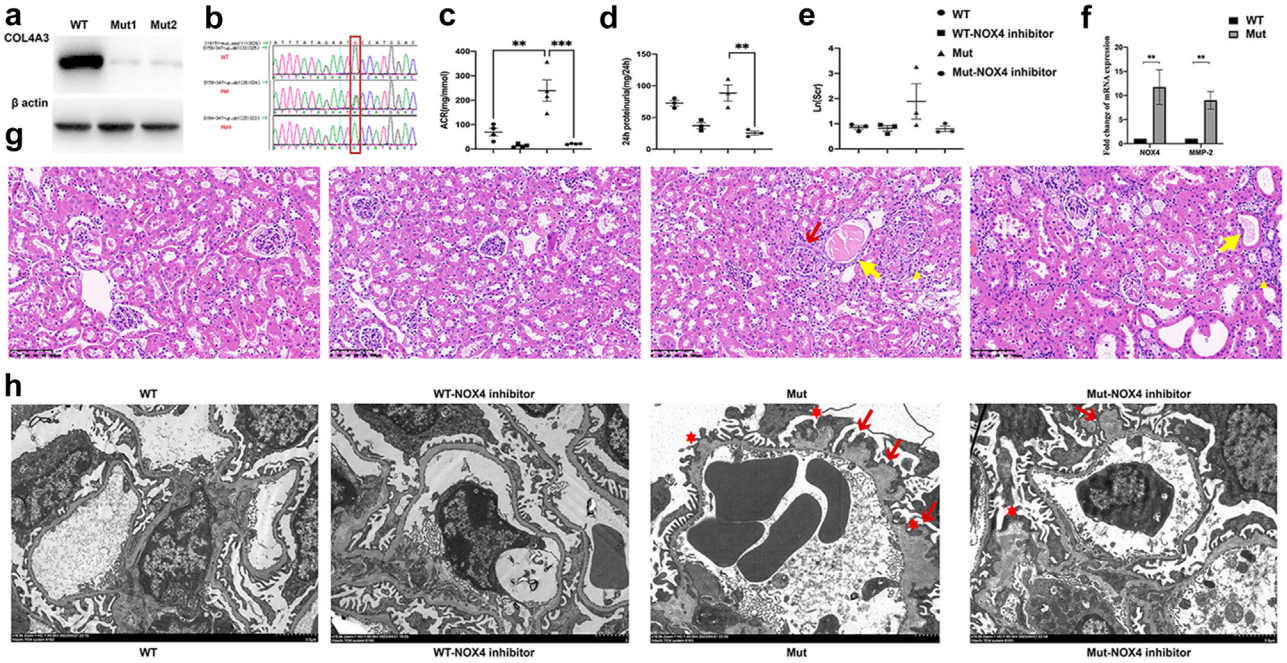

Figure 2. Characterization of *Col4a3* transgenic mouse model. (a) Western blot analysis of type IV collagen α3 chain level in glomeruli of *Col4a3* transgenic mice and wild type (WT) mice. The transgenic group (Mut) had a significantly lower type IV collagen α3 chain level compared with the WT group. (b) Sanger sequencing of *Col4a3* mutant mice constructed by CRISPR/Cas9 technology. (c)–(e) The mutant and WT mice treated with or without NOX4 inhibitor at 28 weeks of age, quantification of urinary ACR ([c] each group $N = 4$), 24 hour proteinuria ([d] each group $N = 3$), serum creatinine ([e] each group $N = 3$, and serum creatinine was transformed as Ln[Scr] because of skewed distribution). $^{**}P < 0.05$, $^{***}P < 0.001$. (f) Real-time PCR validation show the expression of NOX4 and MMP-2 mRNA was higher in mutant group compared with that in WT group. $N = 4$; $^{**}P < 0.01$. (g) Representative light micrographs of HE stained kidney sections from WT and mutant mice at 28 weeks of age. Light micrographs represent focal adhesion of glomeruli (red arrow), tubular cast (yellow arrow), interstitial inflammatory cell infiltration (yellow triangle) in mutant group. $N = 4$. (h) Electron micrographs of kidney tissue from WT and mutant mice at 28 weeks of age. Electron micrographs show partial podocyte foot process effacement (red star), segmental thickening of GBM (red arrow) in mutant group. $N = 4$. ACR, albumin-to-creatinine ratio.

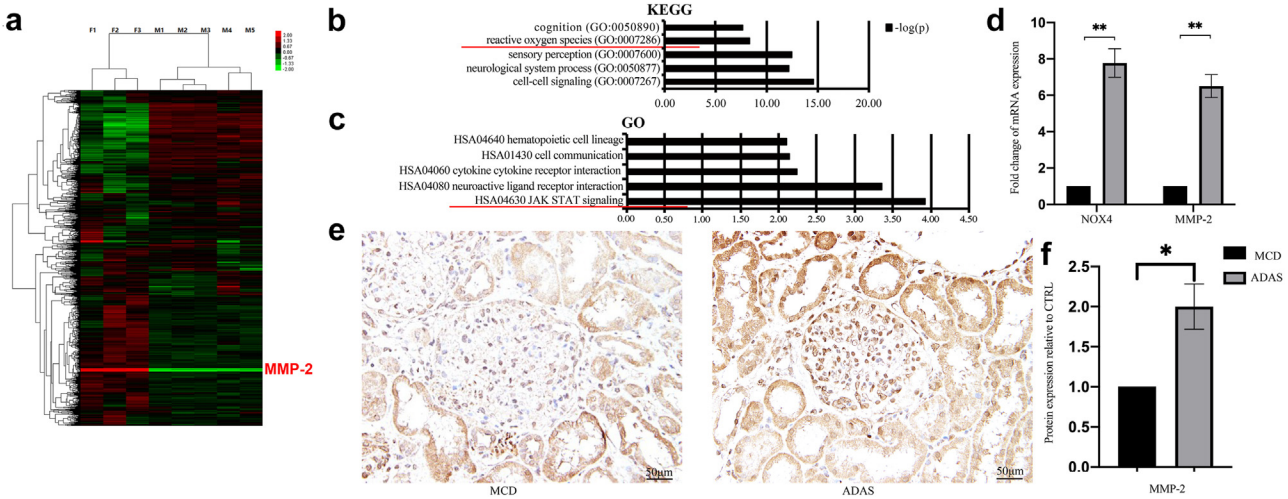

Figure 3. Microarray analysis of patients with ADAS with *COL4A3* mutation followed by validation of DEGs from both transcriptomic and proteomic level. (a) The heat map of gene expression analysis in glomeruli of patients with ADAS and patients with MCD. The line highlighted represents top highest DEG, MMP-2. Red indicates upregulated. Green indicates down-regulated. Black indicates no significant difference between the 2 groups. F1–F3 indicated patients with ADAS with *COL4A3* mutation. M1–M5 indicates patients with MCD as control. (b)–(c) Pathways of genes upregulated in patients with ADAS compared with patients with MCD, using Kyoto Encyclopedia of Genes and Genomes analysis (b), and Enrichr Gene Ontology Biological Process program (c). (d) Real-time PCR validation of NOX4 and MMP-2 in glomeruli of 3 additional patients with ADAS and 7 additional patients with MCD. (e) Immunohistochemical staining of MMP-2 in glomeruli of patients with ADAS and patients with MCD. (f) Histogram of immunohistochemical staining from (e) showed a significant increase in the expression of MMP-2 in glomeruli of patients with ADAS compared with that in glomeruli of patients with MCD. $^{*}P < 0.05$, $^{**}P < 0.01$. $N = 3$. ADAS, autosomal dominant Alport syndrome; MCD, minimal change disease.

with ADAS and 7 additional patients with MCD. The result of real-time PCR suggested that the tendency of *NOX4* and *MMP-2* mRNA expression between the 2 groups was consistent with the microarray results (Figure 3d). We further observed the expression of *MMP-2* was significantly higher in the renal cortex in patients with ADAS compared with the control (patients with MCD) by immunohistochemistry (Figure 3e and f).

Validation of the Relation Between NOX4 and MMP-2

Further, we found the expression of MMP-2 and the level of apoptosis decreased after treating *Col4a3*$^{C1615Y/C1615Y}$ mice with NOX4 inhibitor, GKT137831. However, we confirmed the level of apoptosis decreased, and the expression of NOX4 remained all most the same after treatment with MMP-2 inhibitor, SB-3CT both *in vivo* and *in vitro* (Figure 4a and b). H_2O_2 is the downstream molecule of NOX4, the primary function of NOX4 is to use nicotinamide adenine dinucleotide phosphate to transfer electrons to O_2 molecules to produce H_2O_2,[13] and we found the level of H_2O_2 was higher in *COL4A3* p.C1616Y transgenic podocytes compared with WT podocytes. Next, we inhibited the expression of NOX4 by using GKT137831, and the level of H_2O_2 decreased significantly in *COL4A3* transgenic podocytes (Figure 4c). Histograms represented the difference showing in western blot *in vitro* and *in vivo* separately (Figure 4d and e).

DISCUSSION

COL4(α3/α4/α5) chain is one of the major components of GBM, which is mainly synthesized and secreted by podocytes.[17] Moreover, there is also a small part of COL4 synthesized and secreted by endothelial cells.[18] In our previous work, we identified pathogenetic *COL4A3* mutations segregated in 12.5% of Chinese FSGS families. *COL4A3* mutation-related patients with FSGS presented with different degrees of proteinuria and renal function deterioration; histologic features under electron micrograph included effacement of podocyte foot processes and segmental thinning of the GBM.[19] Based on the advice of the International Alport Cooperation Group, the genetic FSGS caused by the COL4 pathogenetic mutation should be redefined as AS.[20] A majority of studies have reported COL4 mutation results in splitting of the GBM, podocyte foot process effacement, and podocyte apoptosis.[21]

Under physiological conditions, the COL4(α3/α4/α5) chains assemble through recognition of their NC1 domains and form helical heterotrimers in the endoplasmic reticulum of the cell before being secreted into the GBM. Accumulation of abnormal COL4 chains in the endoplasmic reticulum could result in activation of ERS, which has been observed in human podocytes with *COL4A3* G1334E mutation.[22] And in our previous finding, we also observed activation of ERS with subsequent podocyte apoptosis with a truncated *COL4A3* mutation.[12]

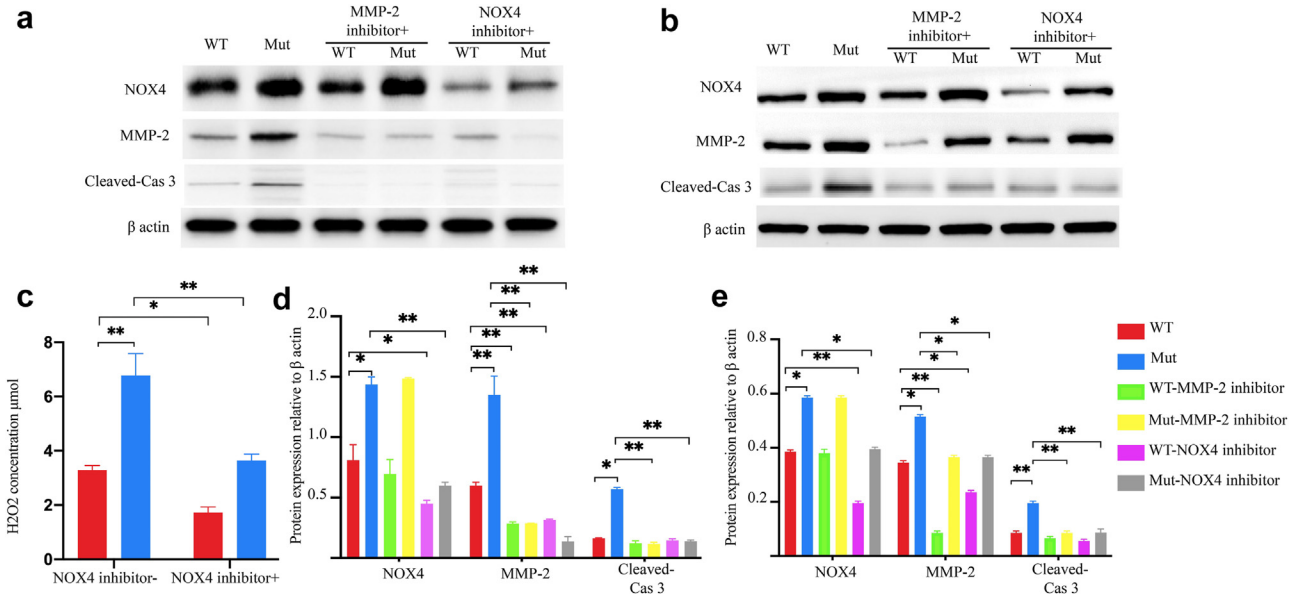

Figure 4. Validation of the relation between NOX4 and MMP-2. (a) In vitro validation, Western blot analysis of NOX4, MMP-2, and apoptosis-related protein cleaved caspase 3 in *COL4A3* transgenic podocytes. (b) In vivo analysis, Western blot verification showed increased expression of NOX4, MMP-2, and cleaved caspase 3 in glomeruli of *Col4a3* transgenic mouse. (c) Measurement of podocyte H_2O_2 before and after NOX4 inhibition. ($N = 4$). (d) Densitometric analysis represented Western blot analysis from (a). ($N = 4$) (e) Densitometric analysis represented Western blot analysis from (b). ($N = 4$) *$P < 0.05$, ** $P < 0.01$.

An increasing number of studies have suggested podocyte apoptosis played a role in diabetic nephropathy (DN). Several studies revealed that hyperglycemia may increase oxidative stress in podocytes, along with the accumulation of ROS, which promote podocyte apoptosis under hyperglycemia.[23] *NOX4* is the major renal source of ROS and is abundantly expressed in podocytes. It is reported that *NOX4* contributes to redox processes involved in DN, acute kidney injury, and hypertensive nephropathy.[24] In addition, researchers reported that podocyte apoptosis was regulated by *NOX4*, major ROS producer in podocytes, and inhibition of NOX4 by Baoshenfang Formula (0.75 g/kg Body Weight, daily, 12 weeks) could decrease proteinuria and protect podocytes from apoptosis under hyperglycemia in DN rats.[25] P53, a well-known pro-apoptotic molecule, is also involved in podocyte apoptosis under hyperglycemia. P53 could cause mitochondrial dysfunction induced by Bcl-2-associated X protein followed by podocyte apoptosis. Down-regulation of NOX4/p53/Bcl-2-associated X protein signaling pathway by huangqi Decoction (1.08 g/kg Body Weight, daily, 8 weeks) could ameliorate podocyte apoptosis induced by hyperglycemia both *in vitro* and *in vivo*.[26] Another study discovered that inhibition of *NOX4* could attenuate renal pathologic change with decreased albuminuria in streptozotocin-induced DN rats, inhibiting podocyte apoptosis, and upregulation of nephrin.[27]

Excessive oxidative stress has been highly emphasized in DN, particularly with extracellular matrix expansion.[28] In this study, we performed microarray analysis of transcripts isolated from the glomeruli of the patients with ADAS, and we found the highest DEG was *MMP-2*. Furthermore, Gene Ontology analysis revealed that one of the top upregulated pathways was JAK-STAT signaling pathway. JAK-STAT pathway controls basic cellular physiologic process, including gene expression, cell activation, proliferation, and differentiation as well as fibrosis.[29] JAK family composes of 4 members, namely JAK1, JAK2, JAK3, and receptor tyrosine kinase 2. And there are 7 STATs, composed of STAT1 to 4, 5a, 5b, and 6.[30] Phosphorylation of JAK activates STAT directly. STAT regulates targeted gene transcription in the nucleus.[31] It is reported that in glomerular diseases such as FSGS, IgA nephropathy, and DN, JAK, STAT, and the inflammatory factors that involved in JAK-STAT signaling were all upregulated.[32] Chen *et al*.[33] explored that high glucose inhibits autophagy by activating JAK-STAT signaling pathway in podocytes, aggravating podocyte injury and accelerating the progression of DN. Oral JAK1/2 inhibitor, LN3103801 administration attenuated pathologic lesion in diabetic mice.[34] Furthermore, inhibition of JAK2 inactivated the downstream STAT4 and Runx3 transcription, followed by inhibition of endothelial cell dysfunction via increasing NO.[35]

MMP-2 is also involved in JAK-STAT signaling pathway. *MMP-2*, a 72kDa type IV collagenase, mainly degrades COL4 in GBM in the kidney. Attachment of podocytes to GBM requires continuous remodeling of COL4, and the process of remodeling needs a moderate level of *MMP-2*, suggesting that *MMP-2* is closely related to the attachment of podocytes to GBM, which is pivotal for the maintenance of podocyte physiological function.[36] It was reported that abnormally upregulated *MMP-2* is closely related to podocyte apoptosis in adriamycin-induced nephropathy,[37] and chronic humoral rejection of human kidney allografts.[38]

NOX4 has been extensively explored in podocyte apoptosis. Guo *et al*.[39] reported that high glucose-induced podocyte apoptosis by upregulating *NOX4*. Liang *et al*.[40] identified that salvianolate could prevent glucose-induced oxidative injury of podocytes through modulation of *NOX4* activity in DN mice. Das *et al*.[41] suggested that TGF-β1 activates *NOX4* in mouse podocyte through Smad2/3 pathways; knockdown of either Smad2 or Smad3 attenuates *NOX4*-induced podocyte apoptosis in DN. Furthermore, activation of mammalian target of rapamycin (mTOR) 1 initiates *NOX4*-dependent podocyte injury in diabetic renal injury.[42] In addition, deletion of *NOX4* decreases albuminuria and attenuates glomerular accumulation of extracellular matrix proteins in streptozotocin-induced diabetic ApoE$^{-/-}$ mice.[43] We found that *NOX4* and ROS were significantly upregulated in patients with ADAS in our study. Furthermore, we discovered a high level of H_2O_2 (major component of ROS) in *COL4A3* transgenic podocytes, which highlighted the correlation between *NOX4* and *MMP-2*. Interestingly, we found the increased level of *MMP-2* and podocyte apoptosis could be rescued after *NOX4* inhibition both *in vivo* and *in vitro*. However, *MMP-2* inhibition could attenuate podocyte apoptosis, but not the level of *NOX4* both *in vivo* and *in vitro*, suggesting that *NOX4* might induce podocyte apoptosis through regulation of *MMP-2* in *COL4A3* mutation.

Luong *et al*.[44] found that phosphate treatment significantly upregulated mRNA level of *NOX4*, and increased expression of downstream *MMP-2* in primary human aortic smooth muscle cells. Diebold *et al*.[45] reported that *NOX4* could upregulate *MMP-2* and stimulate smooth muscle cell proliferation under the stimulation of urotensin-II, a vasoactive peptide associated with vascular remodeling, including congestive heart failure and pulmonary hypertension. And we also found *NOX4* might induce podocyte

apoptosis through regulation of *MMP-2* in *COL4A3* mutation, which was consistent with earlier reports.

There are several limitations in our study, the sample size is relatively small. Because only RNA samples with RNA integrity values >7.0 and RNA concentration >30 ng/μl were qualified for microarray analysis, and more than 500 ng qualified RNA was needed for each sample. In addition, the absence of normal kidney specimens as control group is due to ethical considerations. The nephrectomy samples might not be a good control because the ischemic changes between nephrectomy and biopsy samples are quite different. Therefore, we selected patients with MCD as control. In our study, the level of *NOX4*, *MMP-2*, and cleaved caspase 3 were found to be all upregulated from glomeruli of patients with ADAS. Combined with the interaction between these molecules from our validation *in vivo* and *in vitro*, we suggested that *NOX4*/*MMP-2* pathway can activate cleaved caspase 3 in podocytes in ADAS, and further functional analysis of this pathway needs to be investigated. Our findings suggest that *NOX4*/*MMP-2* pathway may play a key role in the pathogenesis of podocyte apoptosis in ADAS.

CONCLUSION

This study provides a pivotal clue about podocyte apoptosis in patients with ADAS. NOX4/MMP-2/cleaved-Cas 3 pathway was discovered to be activated after *COL4A3* mutation *in vivo* and *in vitro*. These results describe an important pathway involved in podocyte apoptosis in ADAS and help highlight potential novel pharmacologic targets.

DISCLOSURE

The authors have no conflicts of interest to declare.

ACKNOWLEDGMENT

This work was supported by grants from the Major International (Regional) Joint Research Program of National Natural Science Foundation of China (No: 82120108007), the National Natural Science Foundation of China (No.82200790, 81870460, 81570598, 81370015), Program of Shanghai Academic/Technology Research Leader (No: 21XD1402000), Science and Technology Innovation Action Plan of Shanghai Science and Technology Committee (No. 22140904000, 17441902200), Shanghai Municipal Education Commission Gaofeng Clinical Medicine Grant (No.20152207), Shanghai Shenkang Hospital Development Center "Three-year Action Plan for Promoting Clinical Skills and Clinical Innovation in Municipal Hospitals" (No:SHDC2020CR6017), Shanghai Jiao Tong University School of Medicine, Shanghai, China Multi-Center Clinical Research Project (No: DLY201510), Shanghai Jiao Tong University "Jiaotong Star" Plan Medical Engineering Cross Research Key Project(No:YG2019ZDA18) and Shanghai Municipal Key Clinical Specialty(No. shslczdzk02502), Shanghai Jiao Tong University "Jiaotong Star" Plan Medical Engineering Cross Research Project (No:YG2021QN07), and Shanghai Jiao Tong University School of Medicine, 2022 Integrated Traditional Chinese and Western Medicine Research Platform(No: 2022zxy003).

AUTHOR CONTRIBUTIONS

TJ contributed to data collection, analysis and interpretation and wrote the manuscript; ZQM kept the mouse mutants; WQJ assisted in specimen collection; YSW and FZY participated in data analysis; HMJH revised the manuscript; XJ was responsible for kidney biopsy readings; GXC reviewed and revised the manuscript. RH provided substantial guidance; CN and XJY and designed the research and provided substantial guidance.

SUPPLEMENTARY MATERIAL

Supplementary File (PDF)

Table S1. Summary of the clinical characteristics of the patient with ADAS with COL4A3 mutations.

Table S2. Clinical characteristics of patients with ADAS and patients with MCD in the validation group.

REFERENCES

1. Pescucci C, Mari F, Longo I, et al. Autosomal-dominant Alport syndrome: natural history of a disease due to COL4A3 or COL4A4 gene. *Kidney Int.* 2004;65:1598–1603. https://doi.org/10.1111/j.1523-1755.2004.00560.x
2. Gibson J, Fieldhouse Rachel, Melanie M, Chan Y. Omid Sadeghi-Alavijeh, Leslie Burnett, Valerio Izzi, Prevalence Estimates of Predicted Pathogenic COL4A3–COL4A5 Variants in a Population Sequencing Database and Their Implications for Alport Syndrome. JASN. 2021;32(9):2273–2290.
3. Pierides A, Voskarides K, Athanasiou Y, et al. Frequency of COL4A3/COL4A4 mutations amongst families segregating glomerular microscopic hematuria and evidence for activation of the unfolded protein response. Focal and segmental glomerulosclerosis is a frequent development during ageing. *PLoS One.* 2014;9:e115015. https://doi.org/10.1371/journal.pone.0115015
4. Christie SC, Wolock CJ, Groopman E, et al. Exome-based rare-variant analyses in CKD. *J Am Soc Nephrol.* 2019;30:1109–1122. https://doi.org/10.1681/ASN.2018090909
5. Xie J, Chen N. Primary glomerulonephritis in mainland China: an overview. *Contrib Nephrol.* 2013;181:1–11. https://doi.org/10.1159/000348642
6. De Vriese AS, Sethi S, Nath KA, Glassock RJ, Fervenza FC. Differentiating primary, genetic and Sencondary FSGS in adults: a clinicopathologic approach. *J Am Soc Nephrol.* 2018;29:759–774. https://doi.org/10.1681/ASN.2017090958
7. Yao T, Udwan K, John R, et al. Integration of genetic testing and pathology for the diagnosis of adults with FSGS. *Clin J*

Am Soc Nephrol. 2019;14:213–223. https://doi.org/10.2215/CJN.08750718

8. Sachs N, Sonnenberg N. Cell-matrix adhesion of podocytes in physiology and disease. *Nat Rev Nephrol*. 2013;9:200–210. https://doi.org/10.1038/nrneph.2012.291
9. Gorin Y, Cavaglieri RC, Khazim K, et al. Targeting NADPH oxidase with a novel dual Nox1/Nox4 inhibitor attenuates renal pathology in type 1 diabetes. *Am J Physiol Ren Physiol*. 2015;308:F1276–F1287. https://doi.org/10.1152/ajprenal.00396.2014
10. Jha JC, Thallas-Bonke V, Banal C, et al. Podocyte-specific Nox4 deletion affords renoprotection in a mouse model of diabetic nephropathy. *Diabetologia*. 2016;59:379–389. https://doi.org/10.1007/s00125-015-3796-0
11. Zhou G, Wang Y, He P, Li D. Probucol inhibited Nox2 expression and attenuated podocyte injury in type 2 diabetic nephropathy of db/db mice. *Biol Pharm Bull*. 2013;36:1883–1890. https://doi.org/10.1248/bpb.b12-00634
12. Zhang HD, Huang JN, Liu YZ, Ren H, Xie JY, Chen N. Endoplasmic reticulum stress and proteasome pathway involvement in human podocyte injury with a truncated COL4A3 mutation. *Chin Med J (Engl)*. 2019;132:1823–1832. https://doi.org/10.1097/CM9.0000000000000294
13. Li D, Lu Z, Xu Z, et al. Spironolactone promotes autophagy via inhibiting PI3K/AKT/mTOR signalling pathway and reduce adhesive capacity damage in podocytes under mechanical stress. *Biosci Rep*. 2016;36:8–15. https://doi.org/10.1042/BSR20160086
14. Richards S, Aziz N, Bale S, et al. Standards and guidelines for the interpretation of sequence variants: a joint consensus recommendation of the American College of Medical Genetics and Genomics and the Association for Molecular Pathology. *Genet Med*. 2015;17:405–424. https://doi.org/10.1038/gim.2015.30
15. Miller WG, Kaufman HW, Levey AS, et al. National kidney foundation laboratory engagement working group recommendations for implementing the CKD-EPI 2021 race-free equations for estimated glomerular filtration rate: practical guidance for clinical laboratories. *Clin Chem*. 2022;68:511–520. https://doi.org/10.1093/clinchem/hvab278
16. Tong J, Jin Y, Weng Q, et al. Glomerular transcriptome profiles in focal glomerulosclerosis: new genes and pathways for steroid resistance. *Am J Nephrol*. 2020;51:442–452. https://doi.org/10.1159/000505956
17. Gbadegesin RA, Hall G, Adeyemo A, et al. Mutations in the gene that encodes the F-actin binding protein anillin cause FSGS. *J Am Soc Nephrol*. 2014;25:1991–2002. https://doi.org/10.1681/ASN.2013090976
18. Funk SD, Bayer RH, Miner JH. Endothelial cell-specific collagen type IV-α3 expression does not rescue Alport syndrome in COL4A3−/− mice. *Am J Physiol Ren Physiol*. 2019;316:F830–F837. https://doi.org/10.1152/ajprenal.00556.2018
19. Xie J, Wu X, Ren H, et al. COL4A3 mutations cause focal segmental glomerulosclerosis. *J Mol Cell Biol*. 2014;6:498–505. https://doi.org/10.1093/jmcb/mju040
20. Kashtan CE, Ding J, Garosi G, et al. Alport syndrome: a unified classification of genetic disorders of collagen IV α345: a position paper of the Alport Syndrome Classification Working Group. *Kidney Int*. 2018;93:1045–1051. https://doi.org/10.1016/j.kint.2017.12.018
21. Gross O, Licht C, Anders HJ, et al. Early angiotensin-converting enzyme inhibition in Alport syndrome delays renal failure and improves life expectancy. *Kidney Int*. 2012;81:494–501. https://doi.org/10.1038/ki.2011.407
22. Pieri M, Stefanou C, Zaravinos A, et al. Evidence for activation of the unfolded protein response in collagen IV nephropathies. *J Am Soc Nephrol*. 2014;25:260–275. https://doi.org/10.1681/ASN.2012121217
23. Dong XG, An ZM, Guo Y, Zhou JL, Qin T. Effect of triptolide on expression of oxidative carbonyl protein in renal cortex of rats with diabetic nephropathy. *J Huazhong Univ Sci Technol (Med Sci)*. 2017;37:25–29. https://doi.org/10.1007/s11596-017-1689-9
24. Yang Q, Wu FR, Wang JN, et al. Nox4 in renal diseases: an update. *Free Radic Biol Med*. 2018;124:466–472. https://doi.org/10.1016/j.freeradbiomed.2018.06.042
25. Cui FQ, Tang L, Gao YB, et al. Effect of Baoshenfang Formula on podocyte injury via inhibiting the NOX-4/ROS/p38 pathway in diabetic nephropathy. *J Diabetes Res*. 2019;2019:2981705. https://doi.org/10.1155/2019/2981705
26. Chen Y, Chen J, Jiang M, et al. Loganin and catalpol exert cooperative ameliorating effects on podocyte apoptosis upon diabetic nephropathy by targeting AGEs-RAGE signaling. *Life Sci*. 2020;252:117653. https://doi.org/10.1016/j.lfs.2020.117653
27. Zhai R, Jian G, Chen T, et al. Astragalus membranaceus and panax notoginseng, the novel renoprotective compound, synergistically protect against podocyte injury in streptozotocin-induced diabetic rats. *J Diabetes Res*. 2019;2019:1602892. https://doi.org/10.1155/2019/1602892
28. Sen S, Chen SL, Feng BA, Wu YX, Lui E, Chakrabarti S. Preventive effects of North American ginseng (panax quinquefolium) on diabetic nephropathy. *Phytomedicine*. 2012;19:494–505. https://doi.org/10.1016/j.phymed.2012.01.001
29. Balkawade RS, Chen C, Crowley MR, et al. Podocyte-specific expression of Cre recombinase promotes glomerular basement membrane thickening. *Am J Physiol Ren Physiol*. 2019;316:F1026–F1040. https://doi.org/10.1152/ajprenal.00359.2018
30. Brosius FC III, He JC. JAK inhibition and progressive kidney disease. *Curr Opin Nephrol Hypertens*. 2015;24:88–95. https://doi.org/10.1097/MNH.0000000000000079
31. Villarino AV, Kanno Y, O'Shea JJ. Mechanisms and consequences of Jak-STAT signaling in the immune system. *Nat Immunol*. 2017;18:374–384. https://doi.org/10.1038/ni.3691
32. Tao J, Mariani L, Eddy S, et al. JAK-STAT signaling is activated in the kidney and peripheral blood cells of patients with focal segmental glomerulosclerosis. *Kidney Int*. 2018;94:795–808. https://doi.org/10.1016/j.kint.2018.05.022
33. Chen D, Liu Y, Chen J, et al. JAK/STAT pathway promotes the progression of diabetic kidney disease via autophagy in podocytes. *Eur J Pharmacol*. 2021;902:174121. https://doi.org/10.1016/j.ejphar.2021.174121
34. Zhang H, Nair V, Saha J, et al. Podocyte-specific JAK2 overexpression worsens diabetic kidney disease in mice. *Kidney Int*. 2017;92:909–921. https://doi.org/10.1016/j.kint.2017.03.027
35. Jin Q, Lin L, Zhao T, et al. Overexpression of E3 ubiquitin ligase Cbl attenuates endothelial dysfunction in diabetes mellitus by inhibiting the JAK2/STAT4 signaling and Runx3-

mediated H3K4me3. *J Transl Med*. 2021;19:469. https://doi.org/10.1186/s12967-021-03069-w

36. Chen X, Qin Y, Zhou T, et al. The potential role of retinoic acid receptor α on glomerulosclerosis in rats and podocytes injury is associated with the induction of MMP2 and MMP9. *Acta Biochim Biophys Sin (Shanghai)*. 2017;49:669–679. https://doi.org/10.1093/abbs/gmx066
37. Lei FY, Zhou TB, Qin YH, Chen XP, Li ZY. Potential signal pathway of all-trans retinoic acid for MMP-2 and MMP-9 expression in injury podocyte induced by adriamycin. *J Recept Signal Transduct Res*. 2014;34:378–385. https://doi.org/10.3109/10799893.2014.904873
38. Wong W, DeVito J, Nguyen H, et al. Chronic humoral rejection of human kidney allografts is associated with MMP-2 accumulation in podocytes and its release in the urine. *Am J Transplant*. 2010;10:2463–2471. https://doi.org/10.1111/j.1600-6143.2010.03290.x
39. Guo W, Gao H, Pan W, Yu P, Che G. High glucose induces Nox4 expression and podocyte apoptosis through the Smad3/ezrin/PKA pathway. *Biol Open*. 2021;10:bio055012. https://doi.org/10.1242/bio.055012
40. Liang Y, Liu H, Fang Y, et al. Salvianolate ameliorates oxidative stress and podocyte injury through modulation of NOX4 activity in db/db mice. *J Cell Mol Med*. 2021;25:1012–1023. https://doi.org/10.1111/jcmm.16165
41. Das R, Xu S, Quan X, et al. Upregulation of mitochondrial Nox4 mediates TGF-beta-induced apoptosis in cultured mouse podocytes. *Am J Physiol Ren Physiol*. 2014;306:F155–F167. https://doi.org/10.1152/ajprenal.00438.2013
42. Eid AA, Ford BM, Bhandary B, et al. Mammalian target of rapamycin regulates Nox4-mediated podocyte depletion in diabetic renal injury. *Diabetes*. 2013;62:2935–2947. https://doi.org/10.2337/db12-1504
43. Jha JC, Gray SP, Barit D, et al. Genetic targeting or pharmacologic inhibition of NADPH oxidase nox4 provides renoprotection in long-term diabetic nephropathy. *J Am Soc Nephrol*. 2014;25:1237–1254. https://doi.org/10.1681/ASN.2013070810
44. Luong TTD, Schelski N, Boehme B, et al. Fibulin-3 Attenuates Phosphate-Induced Vascular Smooth Muscle Cell Calcification by Inhibition of Oxidative Stress. *Cell Physiol Biochem*. 2018;46(4):1305–1316.
45. Diebold I, Petry A, Burger M, Hess J, Görlach A. NOX4 mediates activation of FoxO3a and matrix metalloproteinase-2 expression by urotensin-II. *Mol Biol Cell*. 2011;22:4424–4434. https://doi.org/10.1091/mbc.E10-12-0971